

# BOUT Simulations of Drift Resistive Ballooning L-mode Turbulence in the Edge of the DIII-D Tokamak

Bruce I. Cohen

Lawrence Livermore National Laboratory, Livermore, CA 94551

in collaboration with

Maxim Umansky, William Nevins, and Mike Makowski  
Lawrence Livermore National Laboratory, Livermore, CA

Jose Boedo and Dmitry Rudakov,, UC San Diego, San Diego, CA

George McKee and Zheng Yan, Univ. of Wisconsin-Madison, Madison, Wisconsin

Rich Groebner and DIII-D Collaboration, General Atomics, San Diego, CA



This work was performed under the auspices of the U.S. Department of Energy by Lawrence Livermore National Security, LLC, Lawrence Livermore National Laboratory under Contract DE-AC52-07NA27344

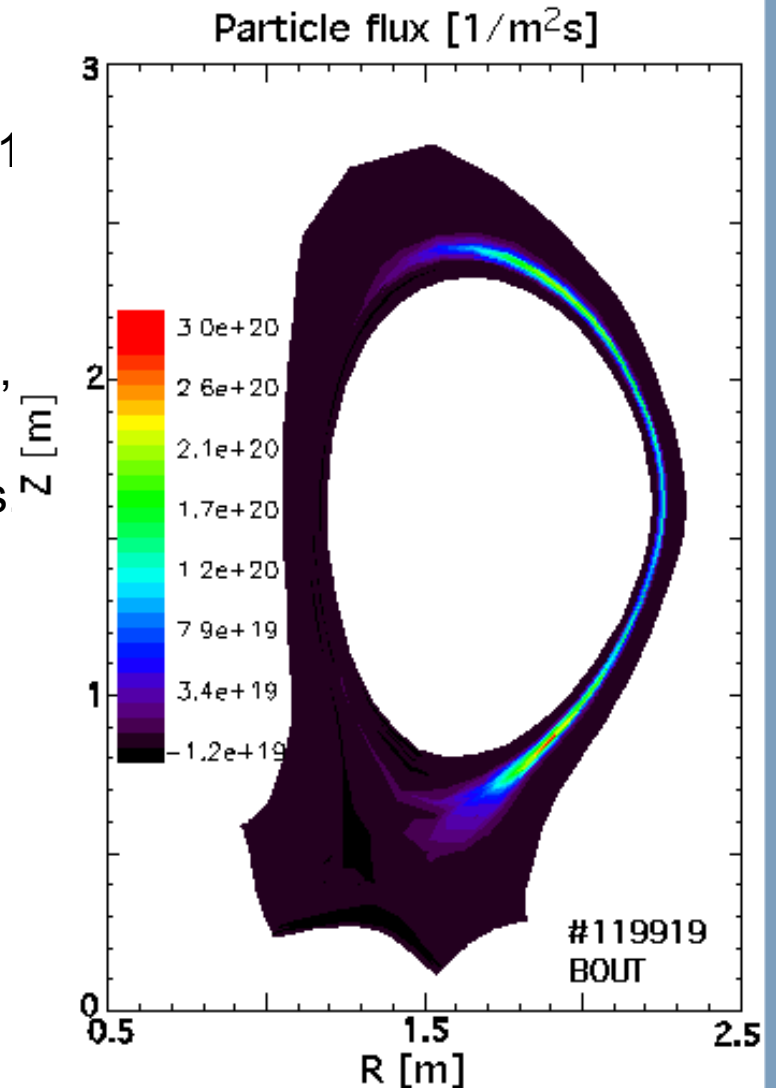
*B. Cohen, et al., APS DPP 2012*

# BOUT Simulations of Drift Resistive Ballooning L-mode Turbulence in the Edge of the DIII-D Tokamak - Outline

1. Introduction -- Overview, definitions of suite of BOUT simulations and equations used
2. BOUT simulations of shot #119919 (with  $T_e$  & with/without  $T_i$  fluctuations)
3. Plunging probe data for shot #119919 and comparison to BOUT simulation
4. BES data for shot #119919, GKV software synthetic diagnostic adjustment for spatial resolution of BES, and comparison to BOUT simulation
5. Inclusion of model  $E_{\text{radial}}(r)$  fitted to probe and CER data in BOUT simulations of #119919: sheared  $E_{\text{radial}} \times B$  is stabilizing
6. Summary of comparisons between BOUT and experimental data from probe and BES for shot #119919
7. Simulations of colder, lower density shot #119934, with and without  $E_{\text{radial}}$
8. Conclusions

# BOUT Simulations of Resistive Drift Ballooning Turbulence in Edge Region for DIII-D Well Characterized L-Mode Shots

- Simulations of electromagnetic resistive drift ballooning in DIII-D L-mode shots #119919, 119921, 119930, and 119934, with full geometry and magnetic shear, crossing the separatrix
- Nonlinear BOUT equations for ion density, vorticity, electron and ion velocities, electron and ion temperatures, Ohm's law, and Maxwell's equations
- **Simulation results for various physics models and validation against probe and BES data**
- **BOUT obtains steady-state turbulence with fluctuation amplitudes and transport that compare reasonably to DIII-D probe and BES data. Sheared rotation due to  $E_{\text{radial}}(r)$  can be stabilizing.**



# Example of Drift Resistive Ballooning Equations in BOUT06

- Consider the following simplified Braginskii + reduced Maxwell eqns with drift ordering in the BOUT06 framework (**Case #4**):

$$\frac{d\tilde{N}_i}{dt} + \nabla N_i \tilde{V}_{\parallel} = \left( \frac{2c}{eB} \right) b_0 \times \kappa \cdot (\nabla \tilde{P}_e - N_i e \nabla \varphi) + \nabla_{\parallel} (\tilde{j}_{\parallel} / e)$$

$$\frac{d\varpi}{dt} = 2\omega_{ci} b_0 \times \kappa \cdot \nabla \tilde{P} + N_{i0} Z_i e \frac{4\pi V_A^2}{c^2} \nabla_{\parallel} \tilde{j}_{\parallel}$$

$$\frac{d\tilde{V}_{\parallel e}}{dt} = -\frac{e}{m_e} E_{\parallel} - \frac{1}{N_{i0} m_e} (T_{e0} \nabla_{\parallel} \tilde{N}_i) + 0.51 v_{ei} \tilde{j}_{\parallel}$$

$$\frac{d\tilde{V}_{\parallel i}}{dt} = -\frac{1}{N_{i0} M_i} \nabla_{\parallel} \tilde{P},$$

$$\frac{d\tilde{T}_e}{dt} = \frac{2}{3N_{i0}} \nabla \cdot (\kappa_{\parallel}^e \nabla_{\parallel} \tilde{T}_e), \quad \kappa_{\parallel}^e = 3.2 \frac{N_{i0} T_{e0} \tau_{e0}}{m_e}$$

$$\mathbf{E} = -\frac{1}{c} \frac{\partial}{\partial t} \mathbf{A}_{\parallel} - \nabla \varphi, \quad -\nabla_{\perp}^2 \mathbf{A}_{\parallel} = \frac{4\pi}{c} \mathbf{j}_{\parallel}, \quad \mathbf{B} = \nabla \times \mathbf{A}_{\parallel} + \mathbf{B}_0$$

$$\varpi = \nabla \cdot [e Z_i N_i \nabla \varphi] \approx e Z_i N_{i0} \nabla^2 \varphi \quad \nabla_{\parallel} = \mathbf{b}_0 \cdot \nabla + \tilde{\mathbf{b}} \cdot \nabla \quad Z_i = 1$$

$$\frac{d}{dt} = \frac{\partial}{\partial t} + (\mathbf{V}_{E0} + \tilde{\mathbf{V}}_E) \cdot \nabla \quad N_i = N_{i0} + \tilde{N}_i, \quad T_s = T_{s0} + \tilde{T}_s, \dots$$

$$\tilde{P} = N_{i0} (\tilde{T}_e + \tilde{T}_i) + \tilde{N}_i (T_{e0} + T_{i0}), \quad T_{i0} = T_{e0}, \quad \tilde{T}_i = 0, \quad V_{\parallel s0} = 0$$

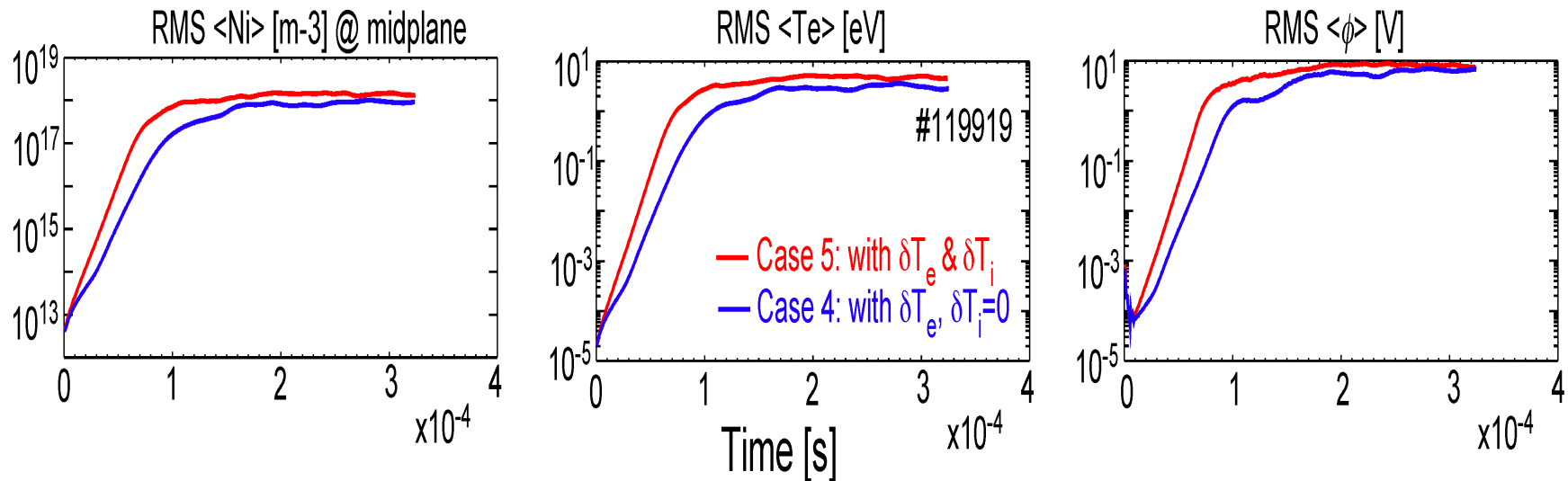
- Electromagnetic with  $\nabla_{\parallel} = \mathbf{b}_0 \cdot \nabla + \tilde{\mathbf{b}} \cdot \nabla$  in  $-\nabla_{\parallel} \phi$  and  $\nabla_{\parallel} \tilde{j}_{\parallel}$
- Actual DIII-D geometry
- Radial bdry conditions: Von Neumann on fluid fluctuations, Dirichlet on  $A_{\parallel}$  &  $\phi$   
Fluctuations decay to 0 at outer bdry & not necessarily at inner bdry
- DIII-D - like fixed background profiles for shots #119919 and 119934
- Case #4** includes  $\delta T_e$  ( $\delta T_i=0$ ) and parallel heat conduction
- Case #5** includes all of the above and evolution equation for  $\delta T_i$

# BOUT Simulation of Resistive Drift Ballooning Turbulence for DIII-D L-mode Shots - Outline

- Electromagnetic simulations of resistive ballooning turbulence in single-null DIII-D geometry (Braginskii equations + drift ordering):
  - Case #1:** Simplest model for resistive drift ballooning ( $\delta T_{e,i}=0$ )
  - Case #2:** Adds  $\delta T_e$
  - Case #3:** Adds  $\delta T_e$  and electron parallel thermal conduction
  - **Case #4:** Adds  $\delta T_e$ , electron parallel thermal conduction, and  $\nabla_{\parallel} = \mathbf{b}_0 \cdot \nabla + \tilde{\mathbf{b}} \cdot \nabla$  in  $-\nabla_{\parallel}\phi$  and  $\nabla_{\parallel}j_{\parallel}$
  - **Case #5:** Adds  $\delta T_e$  and  $\delta T_i$ , etc.
  - **Case #6:** Adds  $\delta T_e$  and  $\delta T_i$ , etc., and imposed  $E_r$
- Comparison to probe and BES data for DIII-D shots #119919,30,34. These shots are well-characterized L-mode shots exhibiting steady-state turbulence.

# History of rms fluctuation amplitudes in midplane at separatrix with electron parallel thermal conduction and magnetic flutter, showing saturated turbulence in BOUT for shot #119919

## BOUT Cases 4 and 5

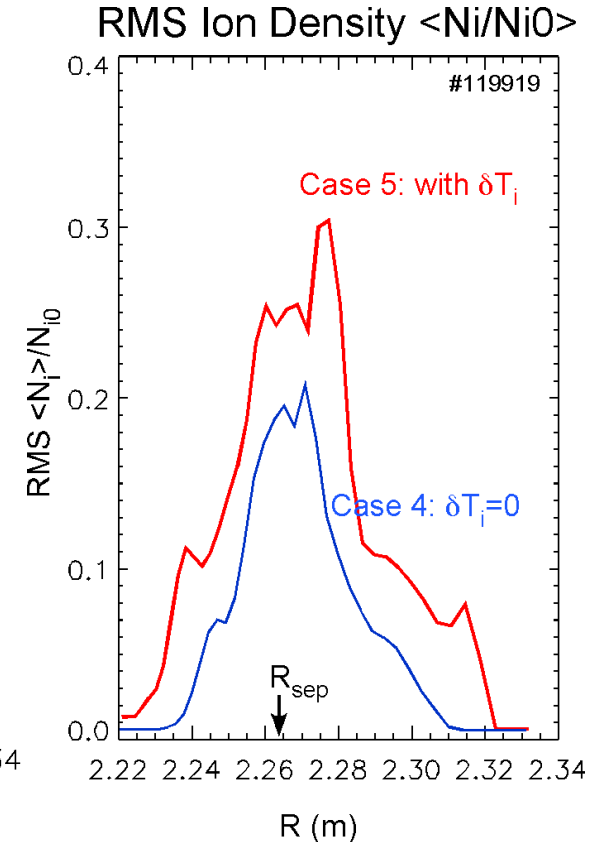
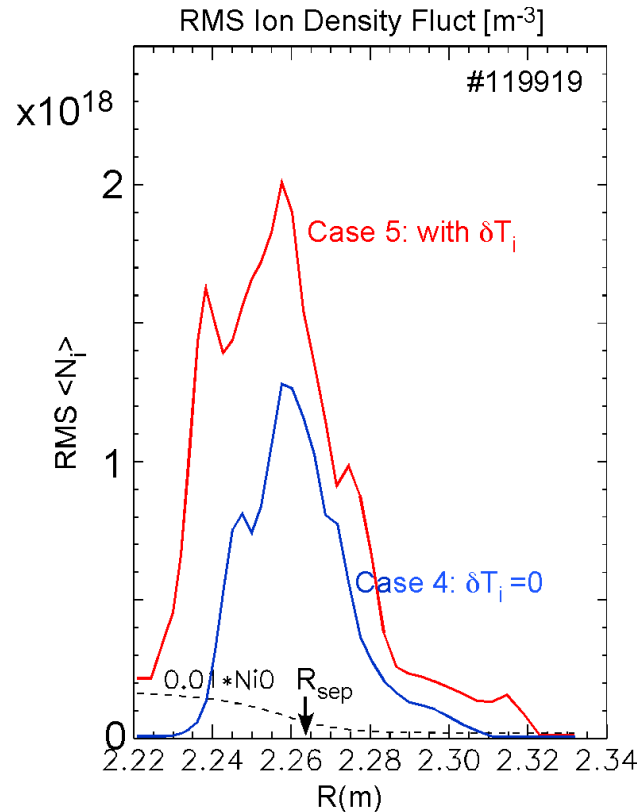
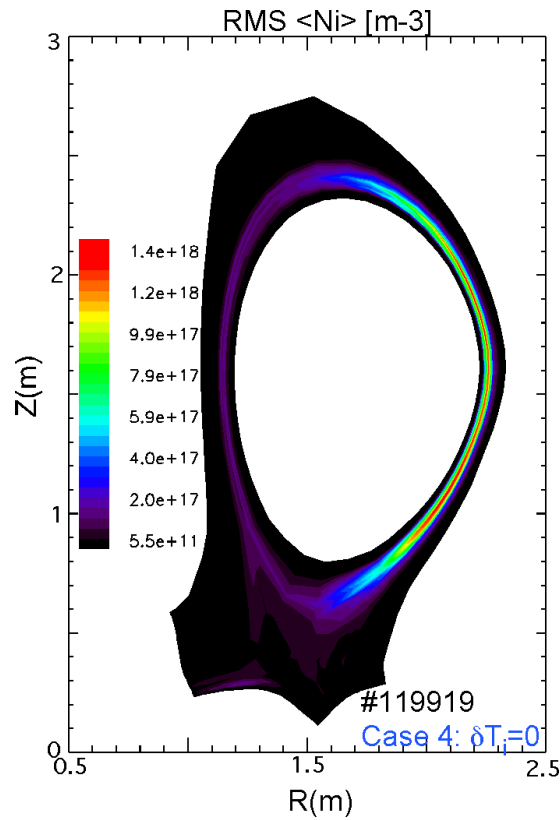


- With  $\delta T_e$ , electron parallel thermal conduction, convective nonlinearities,  
 $\nabla_{\parallel} = \mathbf{b}_0 \cdot \nabla + \tilde{\mathbf{b}} \cdot \nabla$  in  $-\nabla_{\parallel} \phi$  and  $\nabla_{\parallel} j_{\parallel}$  (and  $\delta T_i$  in Case 5)
- Temperature and density fluctuations saturate given fixed background profiles
- Including  $\delta T_i$  increases fluctuation amplitudes modestly

# Time-averaged ion density fluctuations in the midplane saturate at ~10-30% and peak near $R_{\text{sep}}$

BOUT Cases 4 and 5

@ midplane

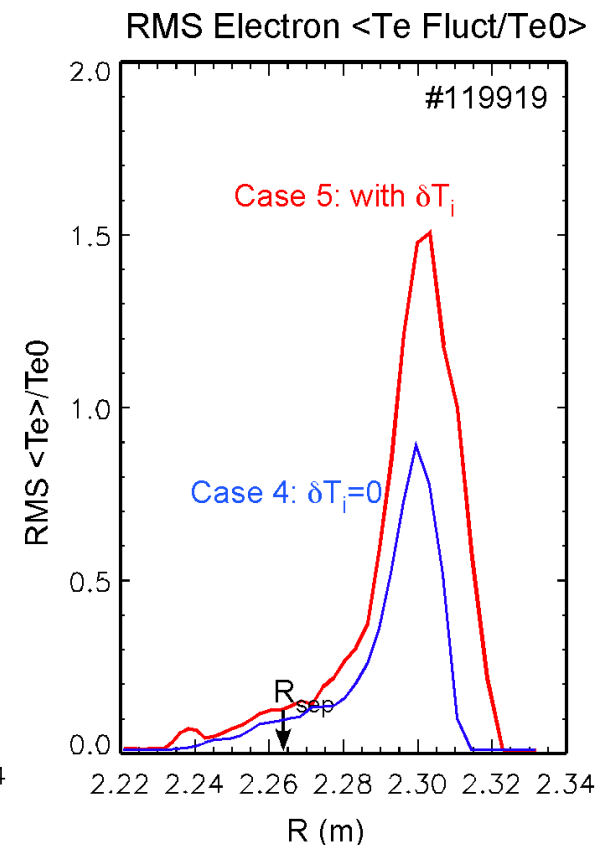
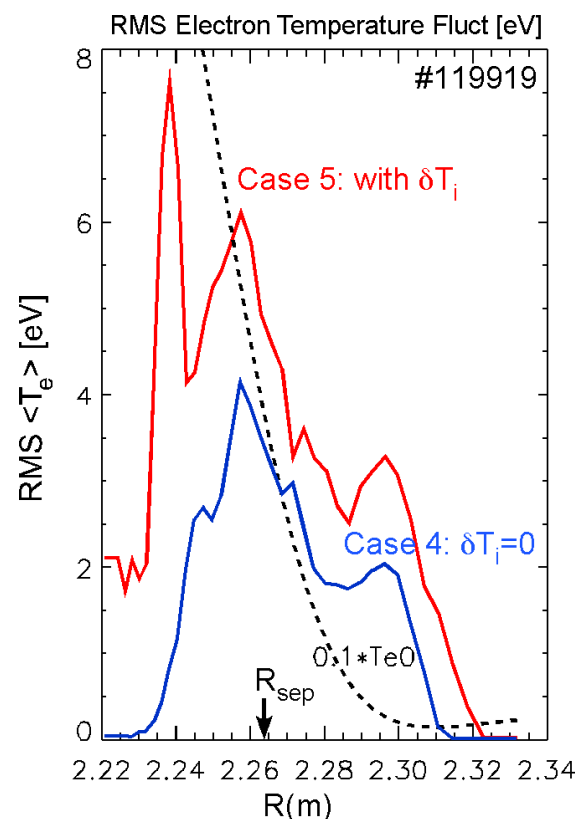
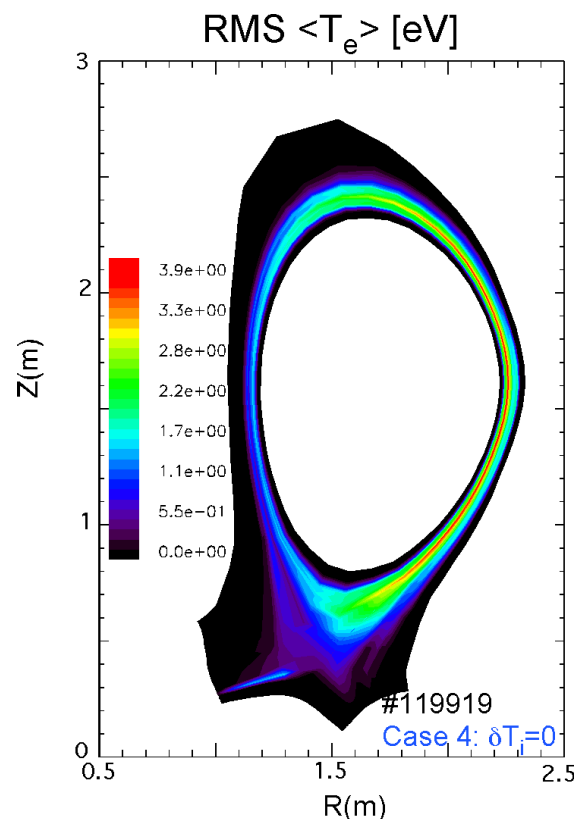


- With  $T_e$  fluctuations, electron parallel thermal conduction, and  $\nabla_{\parallel} = \mathbf{b}_0 \cdot \nabla + \tilde{\mathbf{b}} \cdot \nabla$
- Including  $T_i$  fluctuations leads to ~50% higher fluctuation amplitudes
- There is a poloidal asymmetry wrt midplane in the fluctuations due X-pt & shear

# Time-averaged $T_e$ fluctuations in the midplane peak near the $R_{sep}$ and saturate at $\pm 50\%$ relative amplitude at $R > R_{sep}$

BOUT Cases 4 and 5

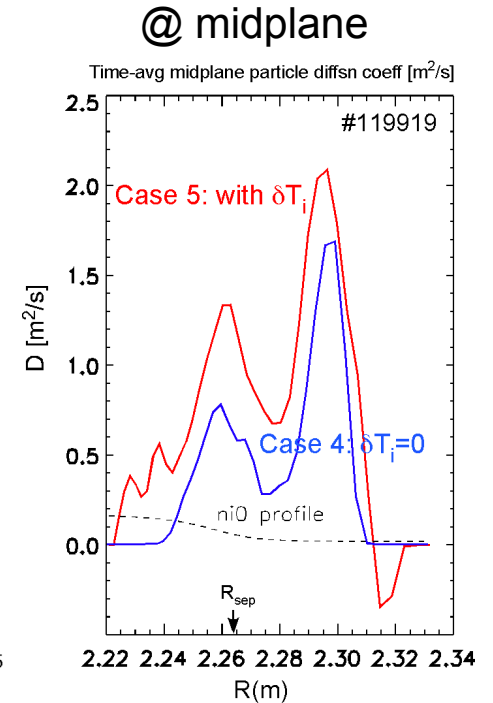
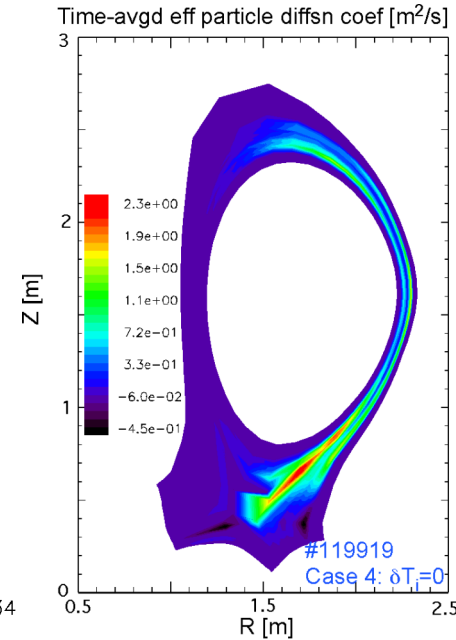
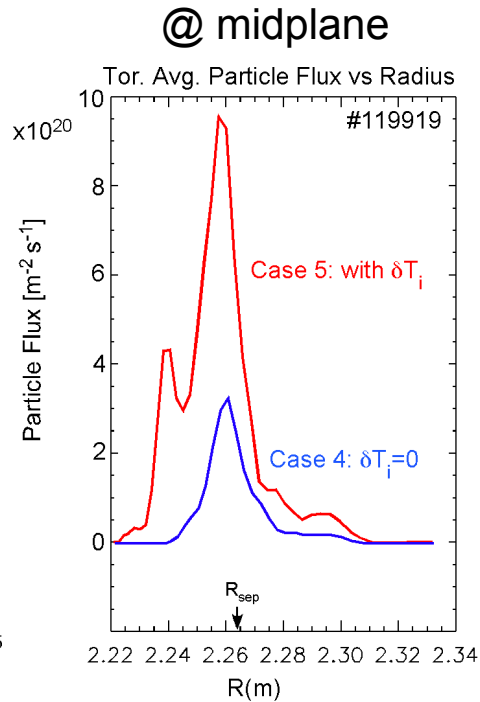
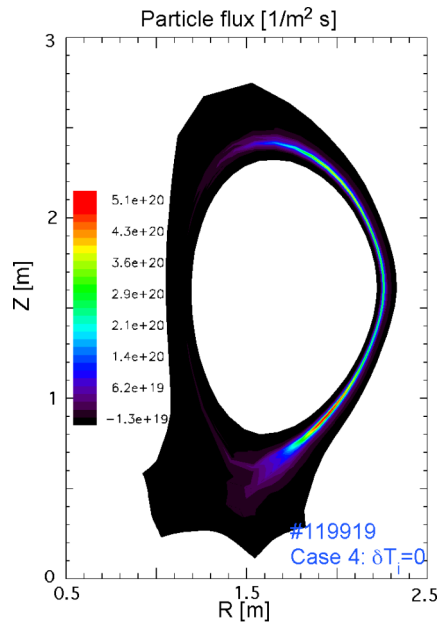
@ midplane



- With  $T_e$  fluctuations, electron parallel thermal conduction, nonlinear convection, and  $\nabla_{||} = \mathbf{b}_0 \cdot \nabla + \tilde{\mathbf{b}} \cdot \nabla$
- $T_e$  fluctuations are  $\sim 10\%$  near  $R_{sep}$  and are generally higher with finite  $\delta T_{ii}$

# Time-averaged ion particle diffusion coefficient in the midplane saturates at $\sim 1.5\text{-}2 \text{ m}^2/\text{s}$

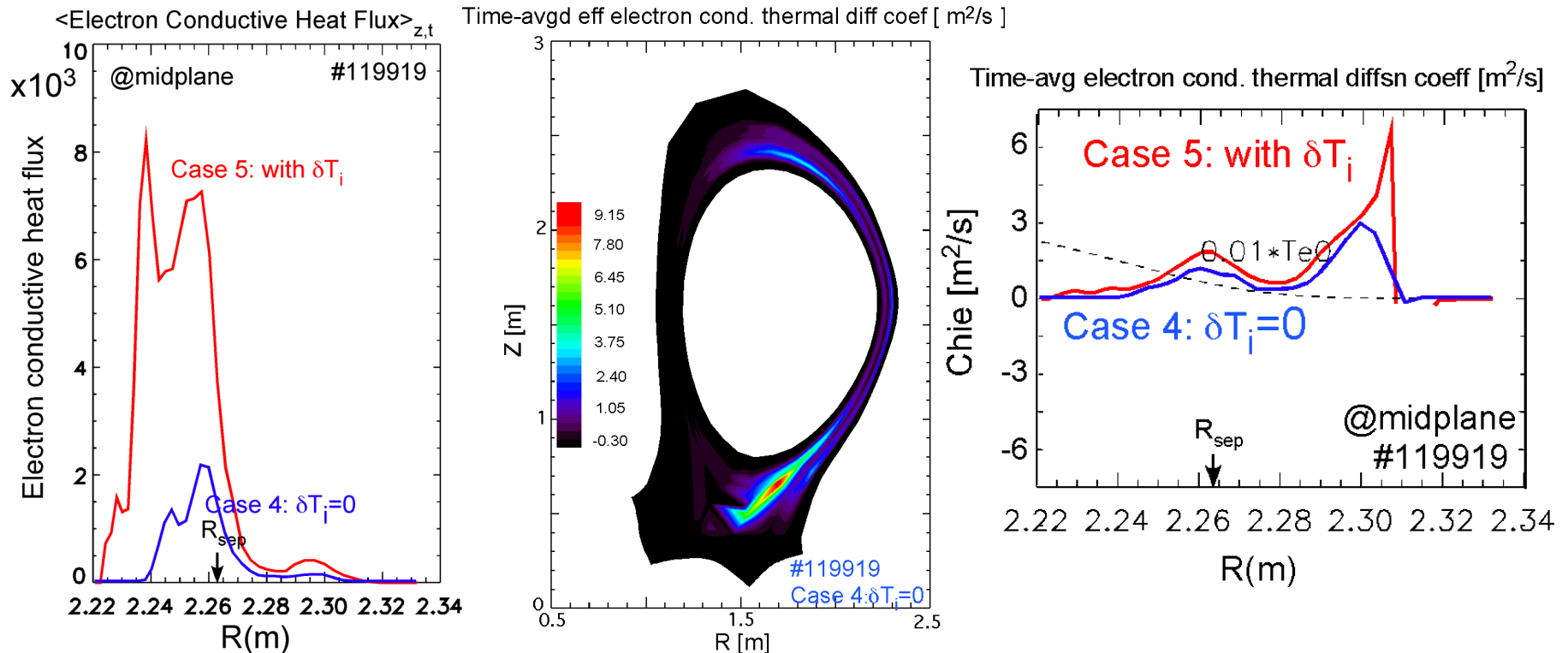
## BOUT Cases 4 and 5



- With  $T_e$  fluctuations, electron parallel thermal conduction, nonlinear convection, and  $\nabla_{\parallel} = \mathbf{b}_0 \cdot \nabla + \tilde{\mathbf{b}} \cdot \nabla$
- Including  $T_i$  fluctuations leads to higher particle fluxes and diffusion coefficient

# Time-averaged electron conductive thermal diffusion coefficient in the midplane saturates at $\sim 2\text{-}6 \text{ m}^2/\text{s}$

## BOUT Cases 4 and 5

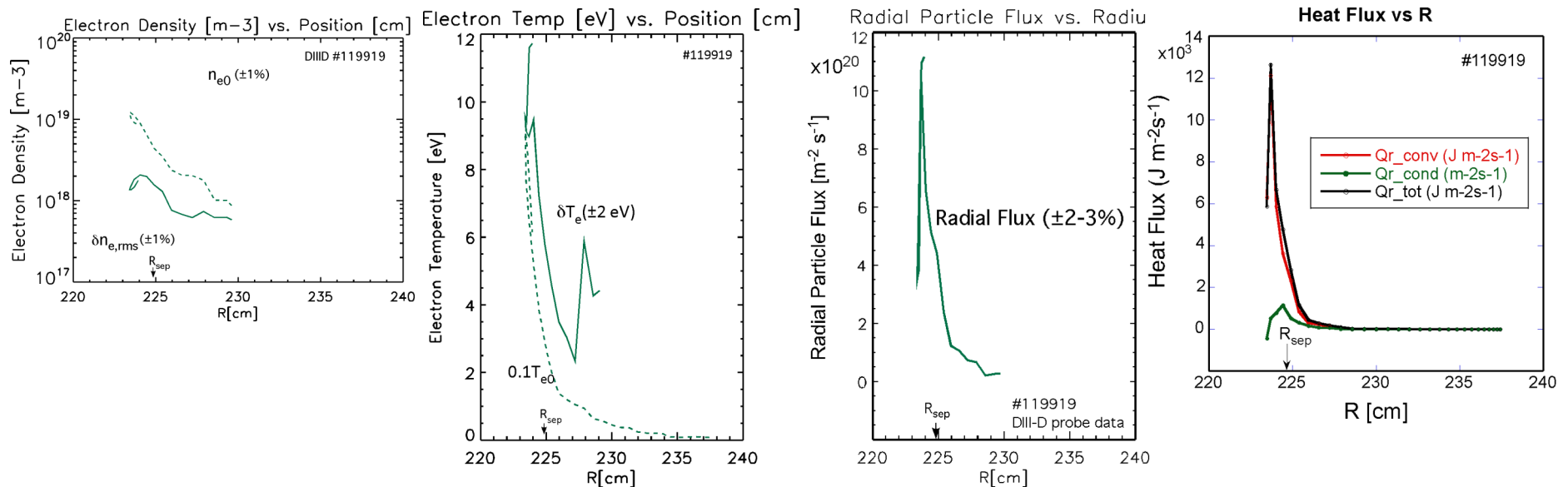


Note: Here heat flux (conductive) =  $\frac{3}{2} N_0 \langle \delta v_r \delta T_e \rangle_{tor,t}$ , and  $\chi_e = -\frac{3}{2} N_0 \langle \delta v_r \delta T_e \rangle_{tor,t} / N_0 \nabla T_{e0}$

- With  $T_e$  fluctuations, electron parallel thermal conduction, nonlinear convection, and  $\nabla_{||} = \mathbf{b}_0 \cdot \nabla + \tilde{\mathbf{b}} \cdot \nabla$
- Including  $T_i$  fluctuations leads to higher heat fluxes and diffusion coefficient

# Langmuir Probe Data for DIII-D #119919 (J. Boedo et al)

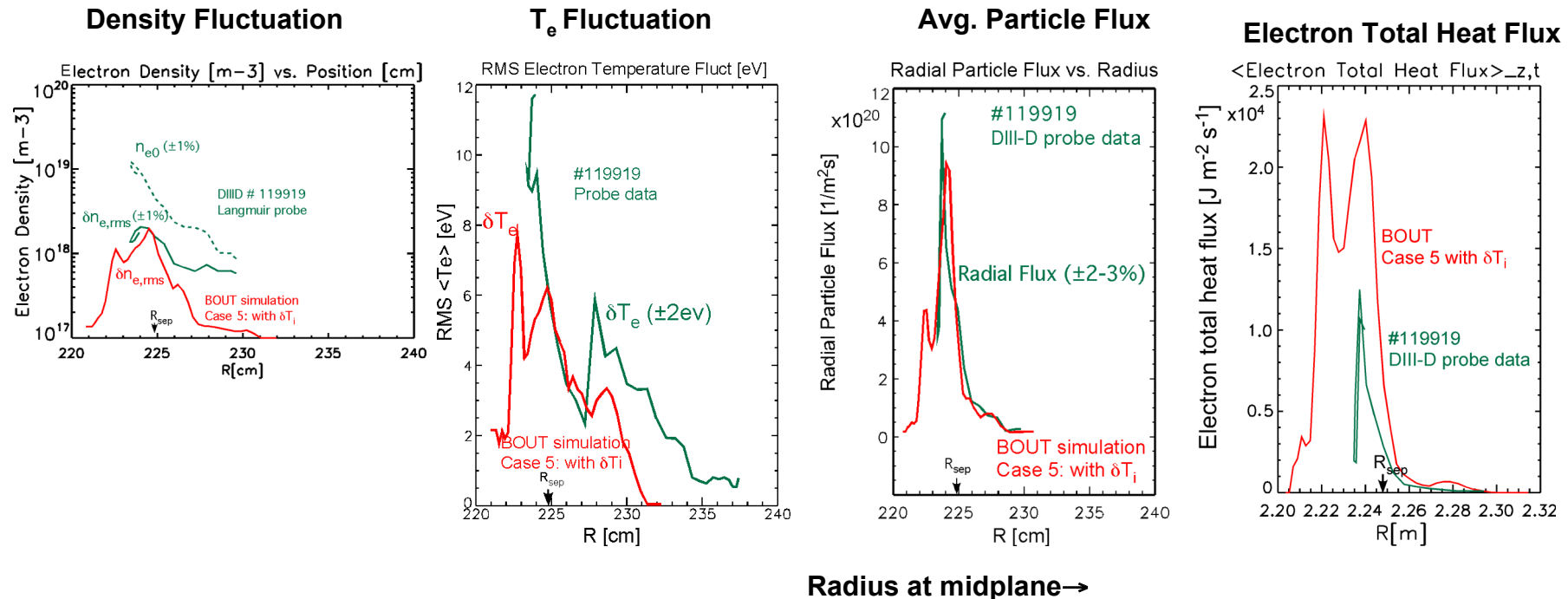
Electron density and radial particle flux vs. radius near midplane -- relative density fluctuations exceed ~20% and temperature fluctuations exceed ~50%



- Probe signals decrease below noise levels for  $R > 229$  cm, and stop for  $R < 223$  cm
- Typical experimental rms  $\delta n_e$  and  $\delta T_e$  fluctuations at the separatrix exceed ~20% & ~50%
- $\delta n_e$ ,  $\delta T_e$  and the probe fluxes in the midplane peak near the separatrix as in BOUT results
- Here the convective heat flux is much larger than the conductive heat flux

There is reasonable agreement between BOUT simulation and Langmuir probe data for DIII-D #119919 with respect to peak fluctuation amplitudes, particle and heat fluxes, and spatial localization

- BOUT with  $T_e$  &  $T_i$  fluct'ns, electron parallel thermal conduction, convective nlrity,  $\nabla_{\parallel} = \mathbf{b}_0 \cdot \nabla + \tilde{\mathbf{b}} \cdot \nabla$

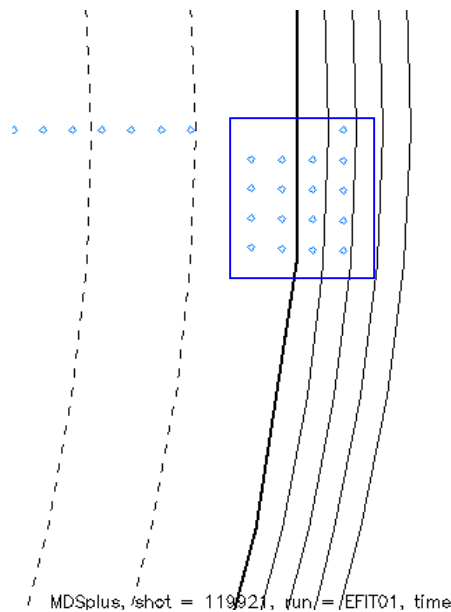


- BOUT simulation results and Langmuir probe data generally agree well on peaking near separatrix and relative spatial localization, and within factors of two on peak amplitudes for density and  $T_e$  fluctuations, and fluxes for  $2.23m \leq R \leq 2.29m$ .
- Agreement on total heat flux is better than on conductive heat flux

# BES Measurements: Long-Wavelength Density Fluctuation Characteristics in 119921-- G. McKee, Z. Yan

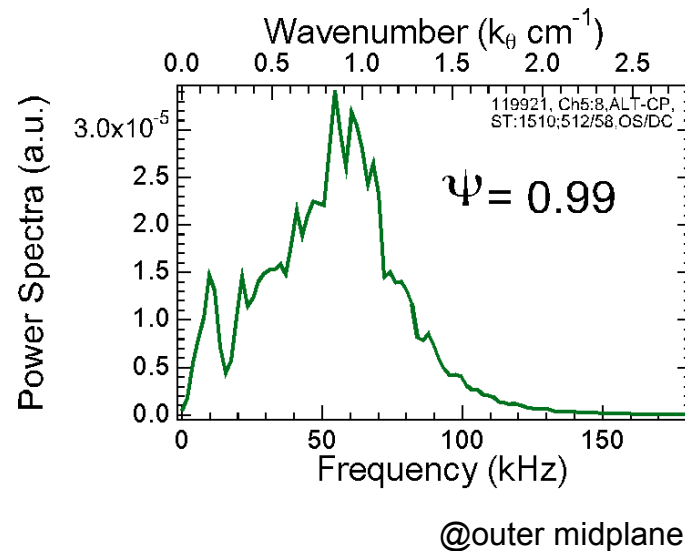
- Short beam-blips injected to obtain BES data during L-mode plasma conditions

BES 4x4 Grid



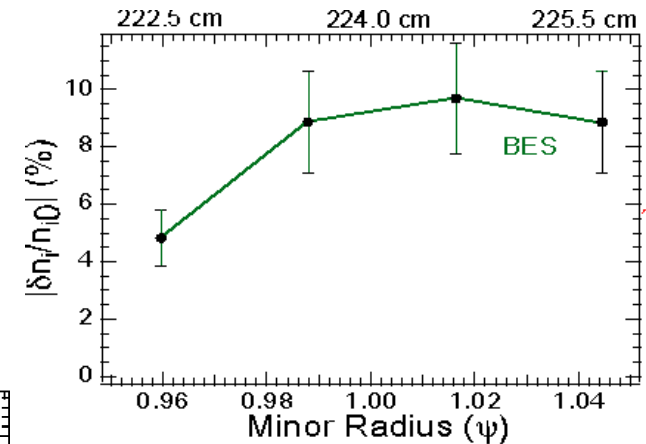
B. Cohen, et al., APS DPP 2012

Density Fluctuation Spectrum

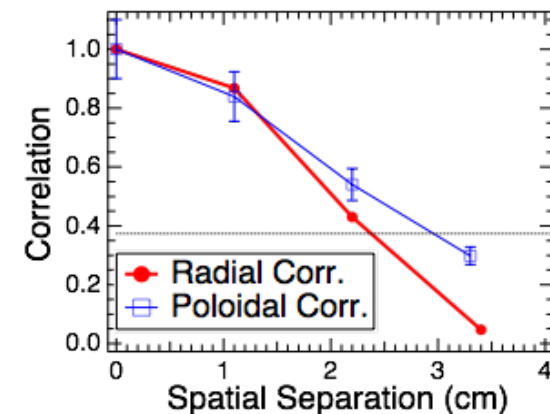


(Preliminary Analysis)

$\tilde{n}/n$  Amplitude Profile



Spatial Correlation



# Synthetic Simulation Diagnostics Using GKV Suite to Match BES Data

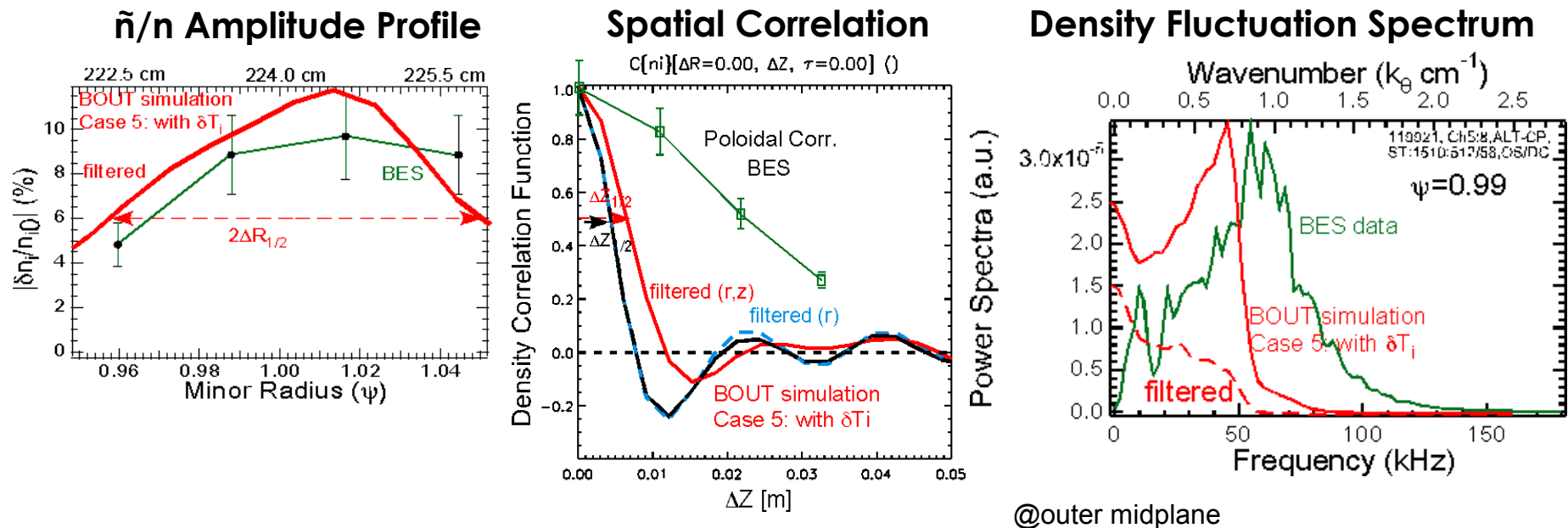
- GKV is a suite of IDL routines built by Bill Nevins to analyze data from simulations or experiments. GKV computes power spectra, correlation functions, etc., makes plots.  
refs: W.M. Nevins, "GKV User's Manual", UCRL-TR-206016 (Aug. 2004); W.M. Nevins *et al.*, Phys. Plasmas **13**, 122306 (2006).
- We construct synthetic diagnostics using the GKV suite of IDL routines to compare to BES data.
- **Spatial filtering** (1D or 2D) required in simulation diagnostics to model the  $\Delta x=1$  cm limit on spatial resolution in the BES grid in R and Z. Filtering is applied to both the radial and binormal coordinates thru the convolution

$$f_{smooth}(x) = \int dx' w(x-x') f(x'), \text{ where } w(x) = \begin{cases} \frac{1}{2\Delta x} \left[ 1 + \cos\left(\frac{\pi x}{\Delta x}\right) \right] & \left| \frac{x}{\Delta x} \right| < 1 \\ 0 & \left| \frac{x}{\Delta x} \right| > 1 \end{cases}$$

- Correlation functions are defined by normalized integrals:

$$C(f; x, t) = \frac{\iint dx' dt' f(x', t') f(x' - x, t' - t)}{\iint dx' dt' f(x', t') f(x', t')}$$

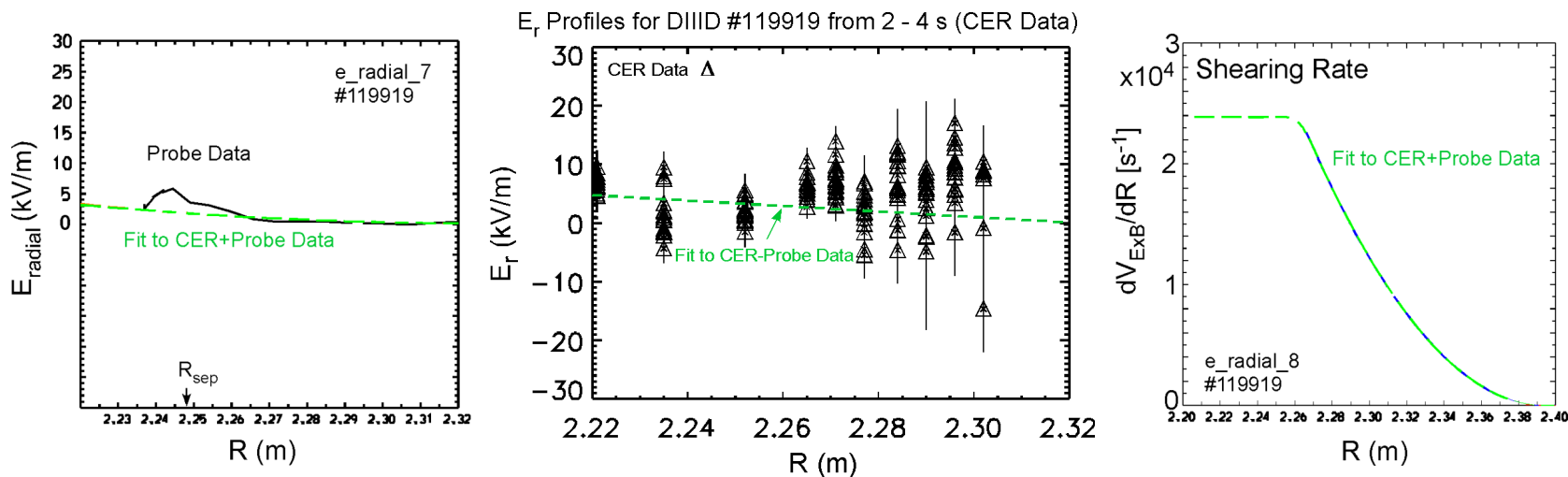
# Reasonable Agreement between BOUT Simulation and BES Data for DIII-D #119921 with respect to Peak Fluctuation Amplitude, Localization, Spatial Correlation Width, and Spectral Width



- Spatial filtering of the BOUT diagnostics reduces and spatially spreads peaks
- There is reasonable agreement between BOUT and BES to within factors of two or three, or less

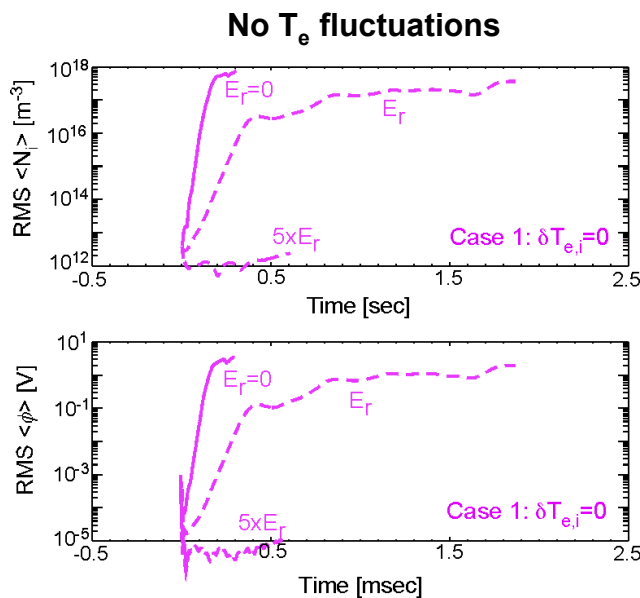
# Model the Experimental Radial Electric Field to Study the Effects of Imposed $E_0 \times B$ Shearing on Simulated Turbulence

- An equilibrium radial electric field  $E_0$  is included in BOUT simulations for Cases 1, 4, & 5, using fits to the experimental probe and CER data near the midplane
- L-mode plasmas typically have weakly sheared  $E \times B$  flows. In our fit to probe and CER data the  $E \times B$  shearing rate is  $< 2.4 \times 10^4$  (1/s)  $<$  BOUT growth rates  $\sim O(1) \times 10^5$  (1/s)
- We expect that with imposed sheared  $E \times B$  flow there will be weaker linear instability and some reduction of the saturated turbulence



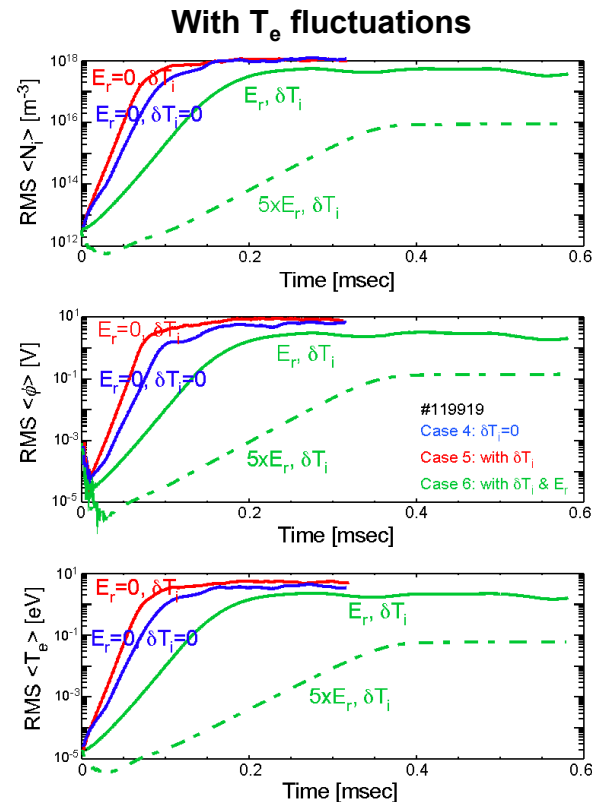
# Imposed $E_0 \times B$ Shearing Reduces Both Linear Growth Rates and Saturated Turbulent Amplitudes

- An equilibrium radial electric field  $E_0$  is included in BOUT simulations for #119919 **Cases 1, 4, 5, & 6**, using fits to the experimental probe and CER data near midplane
- In our fit to probe and CER data the  $E \times B$  shearing rate is  $< 2.4 \times 10^4$  (1/s)  $<$  BOUT growth rates  $\sim O(1) \times 10^5$  (1/s)
- Imposed sheared  $E \times B$  flow weakens linear growth rates, and saturation is much delayed and perhaps at lower amplitudes, while  $5 \times E_r$  is much more stabilized. Have the simulations with  $E_r$  run long enough?



@midplane

B. Cohen, et al., APS DPP 2012



# As the Physics Model Becomes More Complete, the Agreement of BOUT Results with DIII-D Probe Data Improves - Summary

- Comparison of suite of BOUT simulations to shot #119919: peak values in midplane at saturation near  $R_{sep}$  ( $E_{rad}=0$ ,  $E_{rad} \neq 0$ ,  $E_{rad}=5E_{rad}$  with  $\delta T_e$  convective nonlinearity)

Bout simulation	$\langle \delta N_i \rangle_{rms}$ ( $10^{18} m^{-3}$ )	$\langle \delta T_e \rangle_{rms}$ (eV)	Radial Particle Flux ( $10^{20} / m^2 s$ )	$D_r$ ( $m^2/s$ ) local	Conductive Radial Heat Flux $= \frac{3}{2} N_0 \langle \delta \tilde{v}_r \delta \tilde{T}_e \rangle$ ( $10^3 J/m^2 s$ )	$\chi_e$ ( $m^2/s$ ), local conductive
<b>#1</b> : $\delta T_e=0$ $w/E_r^{**}$	0.95 0.37	N/A N/A	1.8 0.07	0.4 0.02	N/A N/A	N/A N/A
<b>#4</b> : $\delta T_e \neq 0$ $\kappa_{  e} \neq 0$ & $\tilde{b} \cdot \nabla$	1.3	4.0	3.3	1.7	3.3	2.7
<b>#5</b> & $w/\delta T_i$	2.0	7.5	9.5	2	10 (total=22)	2.2 (~4)
<b>#6</b> & $w/E_r$ & $w/5E_r$	0.7 0.3	5.5 3.5	0.8 0.18	0.27 0.035	2.5 (4.6) 0.75	0.32 (0.39) 0.036
DIII-D #119919 probe data	2.0	10	11.0	$\sim 0.2-1 \ddagger$	1.2 (total=12)	$\sim 1-2 \ddagger$

\*\*Cases #1  $w/E_r$  has not saturated at end of simulation (1.8 ms) \*total heat flux = cond. +conv. fluxes  
 $\ddagger$ Typical, flux-surface-averaged values for shot #119919 inferred from UEDGE reconstruction

# Comparison of BOUT Results with BES Data for Suite of Physics Models - Summary

- Comparison of suite of BOUT simulations to shot #119921 BES data: fluctuation frequency spectra, peak density amplitude radial half-width, correlation lengths
- Factor of 2 or better agreement seen between **simulation synthetic diagnostics with filtering** and the DIII-D #119921 BES data (with or without sheared  $E_0 \times B$  velocity included in BOUT)

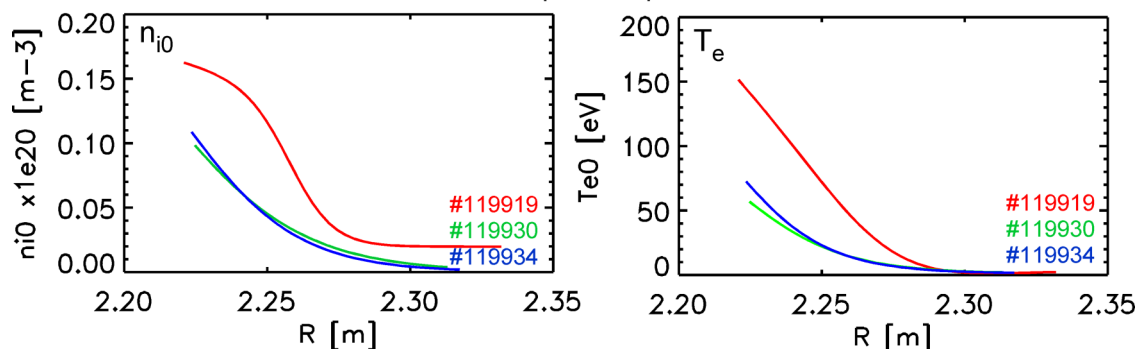
Bout simulation	$\langle \delta N_i / N_i \rangle_{\text{rms}}$ peak vs. R raw/ <b>filtered</b>	$\Delta R_{\text{half-max}}$ of $\langle \delta N_i / N_i \rangle_{\text{rms}}$ (cm) raw/ <b>filtered</b>	$\Delta Z_{\text{corr, half-max}}$ of density (cm) raw/ <b>filtered</b>	Peak freq in density fluct't'n spect, raw/ <b>filtered</b> ( $10^5$ rad/s)	Freq half-max in density fluct't'n spect, raw/ <b>filtered</b> ( $10^5$ rad/s)
<b>#1:</b> $\delta T_e = 0$ $w/E_r^{**}$	0.13 / <b>0.07</b> 0.065/0.045	1.2 / <b>1.5</b> 0.7/0.8	0.6 / <b>0.9</b> 2.0 / 2.3	3 / <b>0.5</b> 0 / 0	4 / <b>2</b> 1/ 0.7
<b>#4:</b> $\delta T_e \neq 0$ $\kappa_{  e} \neq 0$ & $\tilde{\mathbf{b}} \cdot \nabla$	0.20 / <b>0.12</b>	1.4 / <b>1.2</b>	0.4 / <b>0.7</b>	3.0 / <b>1.5</b>	2 / <b>1.2</b>
<b>#5:</b> $w/\delta T_i$	0.21 / <b>0.12</b>	1.7 / <b>2</b>	0.4 / <b>0.7</b>	3.0 / <b>0&amp;1.5</b>	1 / <b>1.5</b>
<b>#6:</b> & $w/E_r$ & $E_r = 5E_r$	0.07 / <b>0.05</b> 0.011/0.006	1.5 / <b>1.7</b> 0.5 / 0.6	0.8/ <b>0.9</b> 3/3	0.5 / <b>0.5</b> 3.8 / 3.8	0.5 / <b>0.5</b> 0.25 / 0.25
DIII-D #119921 BES data	0.09 $\pm$ 0.2	2 $\pm$ 0.2	2 $\pm$ 0.2	3.8	1.3 $\pm$ 0.2

**\*\*Cases #1  $w/E_r$  has not saturated at end of simulation (1.8 ms)**

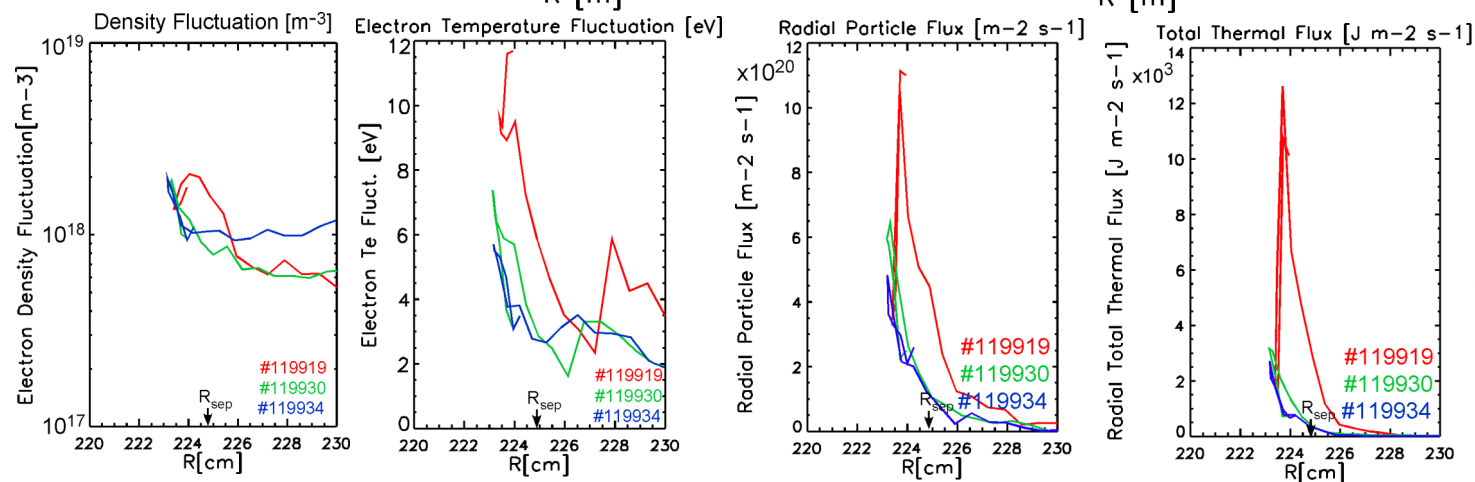
# Comparison of Probe Data from Lower Density and Colder Plasmas in Shots #119930 and 119934 vs. 119919

- Edge plasmas in L-mode shots #119930 and 119934 are colder and have lower densities than in shot #119919
- The growth rate for resistive ballooning is proportional to  $\eta^{1/3} \beta^{2/3} / n^{1/3} \propto T^{1/6} n^{1/3}$
- A factor of two lower temperature and density decreases the drive for resistive ballooning by  $O(1/\sqrt{2})$  if all else is fixed in shots #119930/119934 vs. #119919

Outer midplane profiles



$N_{i0}$  &  $T_{e0}$  profiles



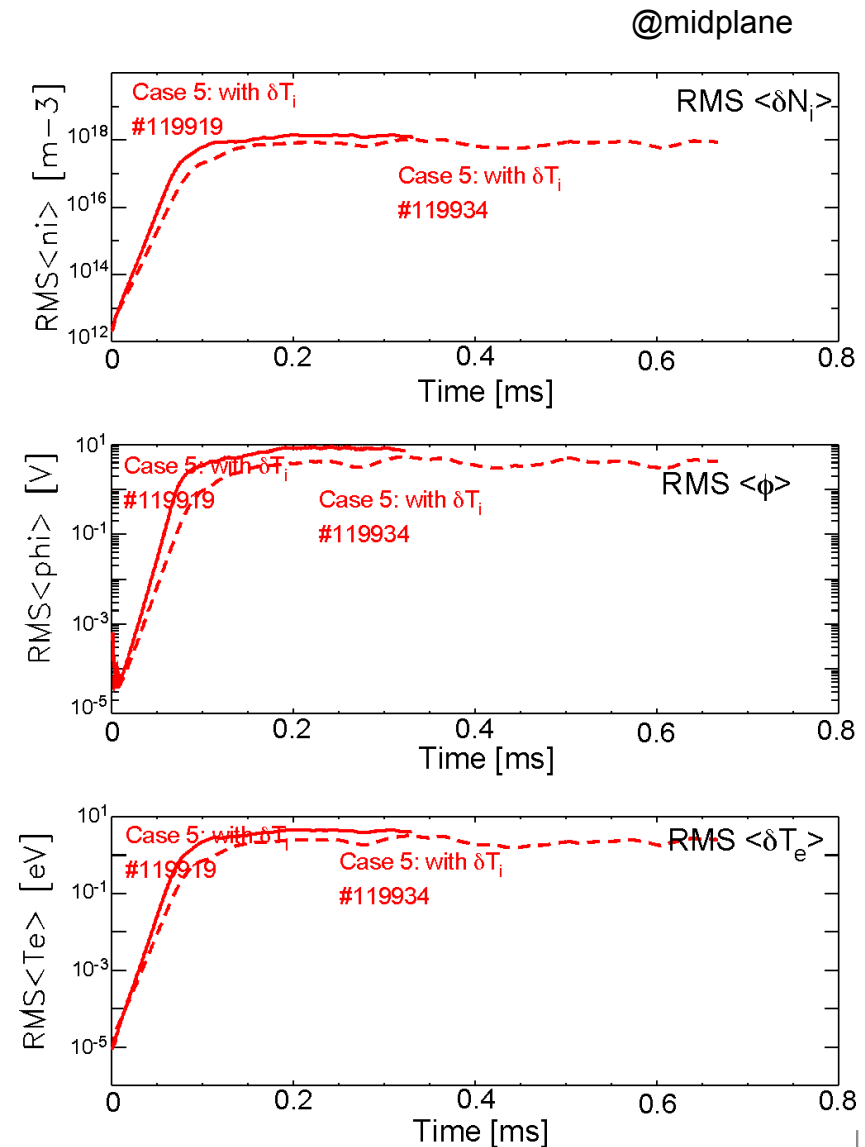
Probe data

Reduced  $N_{i0}$  &  $T_{e0}$  lead to **reduced fluctuation amplitudes and radial fluxes** in #119930 & 119934

@midplane

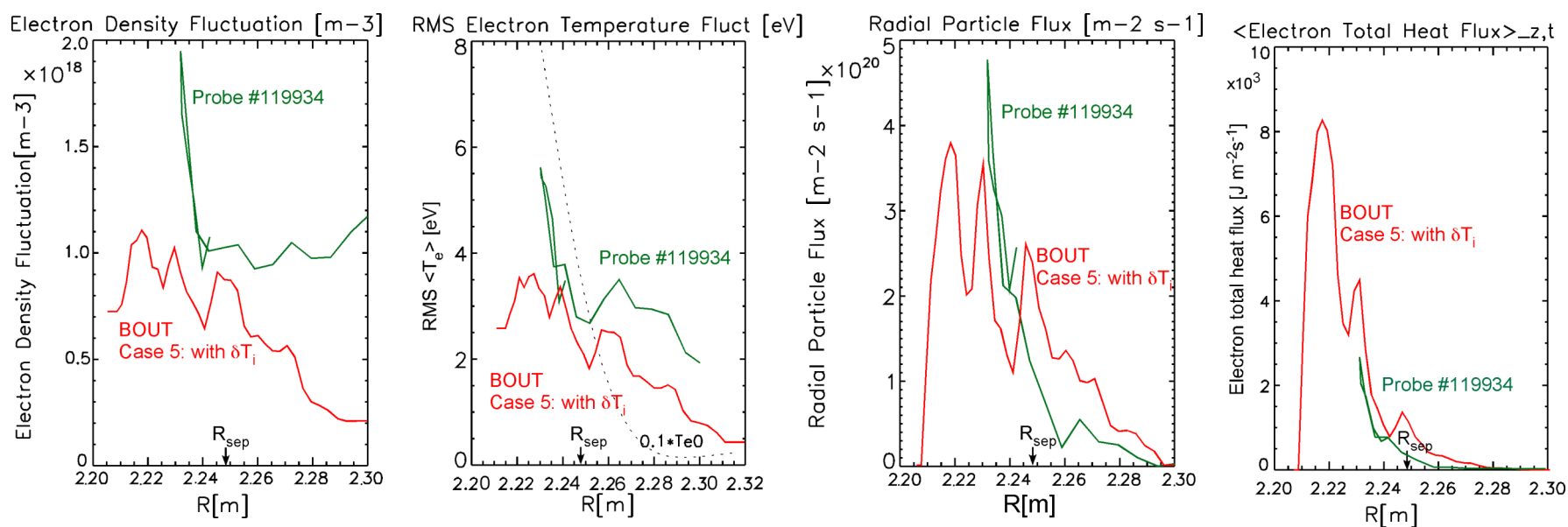
# BOUT Simulations of Shots #119919 and 119934 Show Reduced Turbulence with Lower Equilibrium Temperature and Density

- BOUT simulations of **Case 5** with no  $E_{\text{radial}}$  for shots # 119919 and 119934 show that the linear growth rate for the resistive-drift ballooning instability is reduced by  $\sim 20\%$  in 119934, roughly consistent with inference from the linear dispersion relation for resistive ballooning
- The absolute values of the fluctuation amplitudes are reduced in #119934 accompanying the reduction in growth rate of the instability



# Agreement of BOUT Simulation with Probe Data for Shot #119934 Is Similar to Agreement Seen for Shot #119919

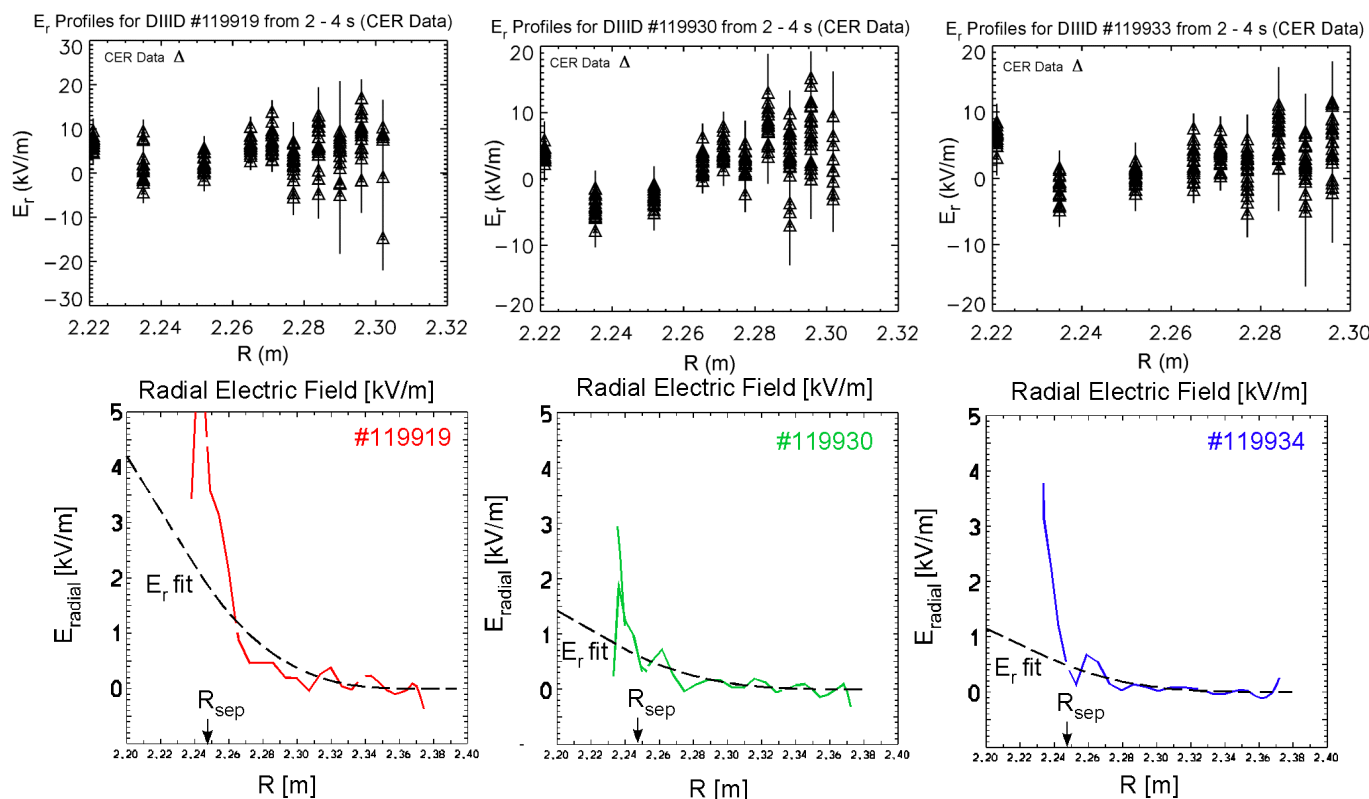
- Probe data from L-mode shot #119934 is compared with BOUT simulation including  $T_e$  and  $T_i$  fluctuations (**Case 5**). Turbulence in #119934 is reduced from that in #119919
- Density and temperature fluctuations, and radial fluxes tend to peak near the separatrix
- Saturated density and  $T_e$  fluctuations, and electron particle and total thermal fluxes agree with probe data within factors of  $\sim 2$  for  $2.23\text{m} \leq R \leq 2.29\text{m}$



Case 5 #119934

# Radial Electric Fields Fitted to Probe and CER Data for Simulations of Shots #119919, 119930 and 119934

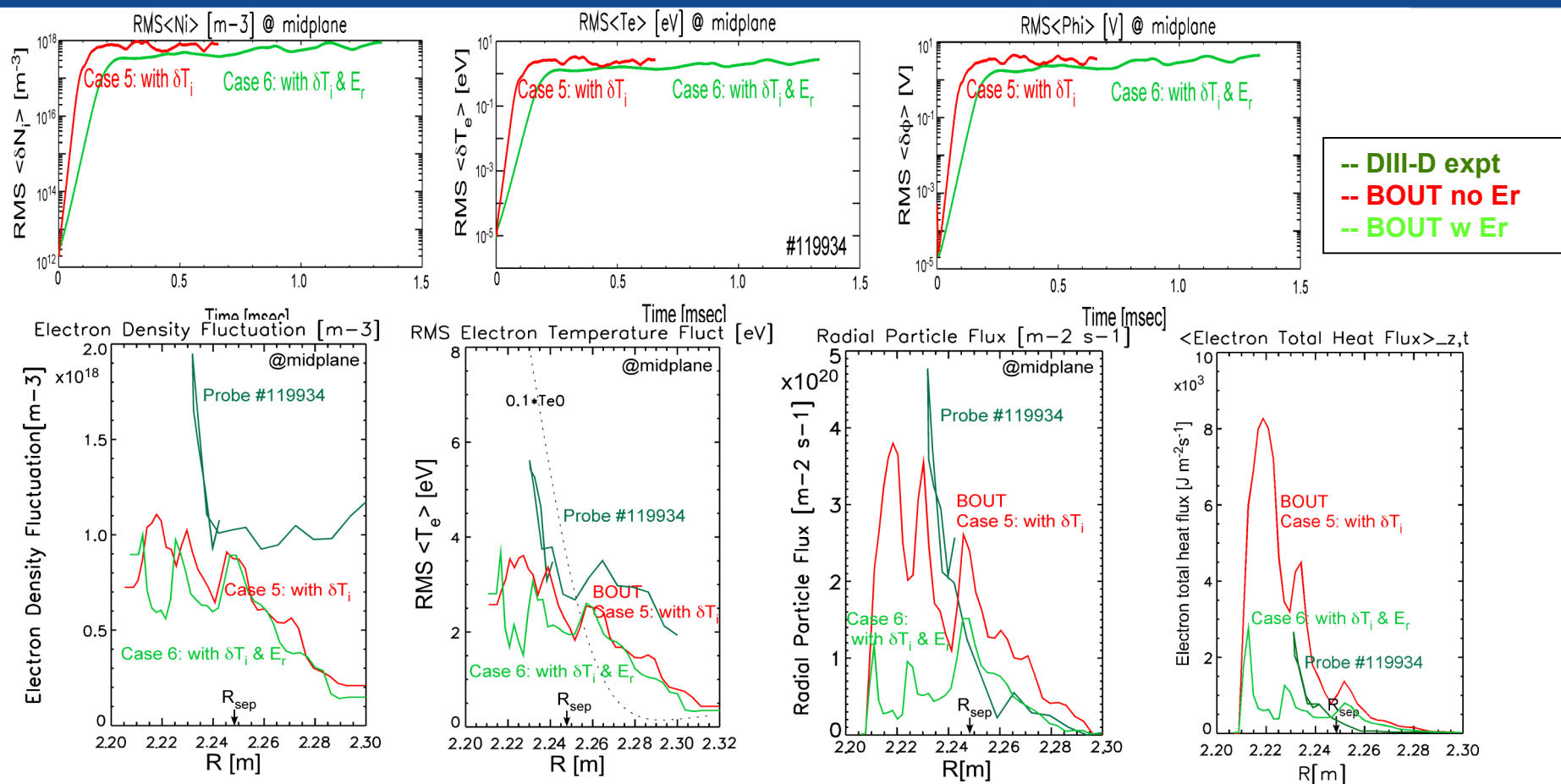
- The electric potential and radial electric field are well determined from the probe data in the SOL, but have a lot of structure inside the last close flux surface.
- The radial electric field determined by CER extends to smaller radii and suggests that  $E_r$  is relatively flat within significant temporal scatter.
- Our model preserves 1st and 2nd radial derivatives of  $\phi$  across  $R_{sep}$ . Alternative models for  $E_r$  need to be studied. Self-consistent zonal flows will be included.



$E_{radial}$  CER data

$E_{radial}$  probe data & fit to probe/CER data

# Inclusion of $E_r$ Reduces Growth Rates but Fluctuation Levels Recover to Near Levels for $E_r=0$ in Simulation of Shot #119934



- Inclusion of  $E_r$  reduces linear growth rates, but fluctuation amplitudes slowly rise to near those with  $E_r=0$ .
- Simulation agreement with probe for  $2.23m \leq R \leq 2.29m$  remains reasonably good with/without  $E_r$

B. Cohen, et al., APS DPP 2012

## Summary: Relative Agreement in Comparison of BOUT Results with DIII-D Probe and BES Data on Shots #119919/..21/..34...

- Comparison of suite of BOUT simulations to shots #119919/119921 probe and BES data -- fluctuation frequency spectra, peak density amplitude radial half-width, correlation lengths, fluxes and diffusion rates are in reasonable agreement.
- RMS peak density and temperature fluctuation amplitudes measured with Langmuir probe agree (#119919 & 119934) within factors of 2 or less with simulations as the physics model improves. Observed radial particle diffusivities and thermal diffusivities in simulation are consistent with typical L-mode inferred values.
- Spatial filtering of synthetic simulation diagnostics is needed to model the 1 cm spatial resolution of the BES data. The spatial filtering spreads and reduces peaks in the raw data.
- There is factor-of-2 or better agreement seen between simulation synthetic diagnostics and the DIII-D #119921 BES data for the relative ion density and  $T_e$  fluctuation amplitudes, particle flux, spatial widths, and spectral frequency widths.
- Inclusion in simulation of radial  $E_r$  modeling expt introduces sheared ExB flow that reduces growth rates, and reduces saturation amplitudes in simulation of #19 but *not* in #34. More work is in progress to understand the effects of  $E_r$  and self-consistent zonal flows.
- Colder, lower density edge plasmas are less unstable and have smaller fluctuation levels.
- **Resistive drift ballooning modes are a reasonable candidate for L-mode edge plasma turbulence in DIII-D shots.**